A Lagrangian Approach for Electrostatic Analysis of Deformable Conductors

Gang Li and N. R. Aluru, *Member, IEEE*

***Abstract*—Deformable conductors are frequently encounted in microelectromechanical systems (MEMS). For example, in electrostatic MEMS, microstructures undergo deformations because of electrostatic forces caused by applied potentials. Computational analysis of electrostatic MEMS requires an electrostatic analysis to compute the electrostatic forces acting on micromechanical structures and a mechanical analysis to compute the deformation of micromechanical structures. Typically, the mechanical analysis is performed by a Lagrangian approach using the undeformed position of the structures. However, the electrostatic analysis is performed by using the deformed position of the conductors. In this paper, we introduce a Lagrangian approach for electrostatic analysis. In this approach, when the conductors undergo deformation or shape changes, the surface charge densities on the deformed conductors can be computed without updating the geometry of the conductors. The Lagrangian approach is a simple, but critical, idea that radically simplifies the analysis of electrostatic MEMS. [715]**

I. Motivation

COMPUTATIONAL analysis of electrostatically actuated MEMS requires a self-consistent solution of the coupled mechanical and electrical equations [1]–[3]. To understand the current approach for self-consistent analysis of electrostatic MEMS, consider the simple example, a cantilever beam over a ground plane, shown in Fig. 1. When a voltage is applied between the cantilever beam and the ground plane, electrostatic charges are induced on the surface of the conductors. These charges give rise to electrostatic forces, which act normal to the surface of the conductors. Since the ground plane is fixed and cannot move, the electrostatic forces deform only the cantilever beam. When the beam deforms, the charge redistributes on the surface of the conductors and, consequently, the resultant electrostatic forces and the deformation of the beam also change. This process continues until an equilibrium state is reached. The primary steps involved in the self-consistent solution approach are summarized in Algorithm 1.

Manuscript received July 9, 2001; revised November 15, 2001. This work was supported by a grant from DARPA under Agreement F30602-98-2-0178. The work of N. R. Aluru was supported by an NSF CAREER award. Subject Editor G. Stemme.

G. Li is with the Department of Mechanical and Industrial Engineering, Beckman Institute for Advanced Science and Technology, University of Illinois at Urbana-Champaign, Urbana, IL 61801 USA.

N. R. Aluru is with the Department of General Engineering, Beckman Institute for Advanced Science and Technology, University of Illinois at Urbana-Champaign, Urbana, IL 61801 USA (e-mail: aluru@uiuc.edu).

Publisher Item Identifier S 1057-7157(02)04990-9.

Algorithm 1 Procedure for coupled electromechanical analysis

repeat

1. Do mechanical analysis (on the undeformed geometry) to compute structural displacements
2. Update the geometry of the conductors using the computed displacements
3. Compute surface charge density by electrostatic analysis (on the deformed geometry)
4. Compute electrostatic forces (on the deformed geometry)
5. Transform electrostatic forces to the original undeformed configuration

until an equilibrium state is reached

In Algorithm 1, initial or undeformed configuration refers to the configuration shown in Fig. 1(a). As the name implies, the undeformed configuration refers to the position of the conductors before any deformation has taken place. Deformed configuration refers to the position of the system after one or more structures have undergone a deformation. For example, shown in Fig. 1(b) is a deformed configuration of the system when the beam has undergone a deformation. It is important to note that a deformed configuration does not necessarily refer to the final equilibrium position of the structure for an applied voltage. It could simply be an intermediate deformed state before a final deformation or an equilibrium state is reached. The two primary steps in Algorithm 1 are mechanical and electrostatic analyzes. Mechanical analysis is performed to compute the deformation of the structures given electrostatic forces. Electrostatic analysis is performed to compute the surface charge densities and the electrostatic forces. Mechanical analysis is typically implemented using the initial or the undeformed configuration. When the structural displacements are computed using the mechanical analysis, the geometry of the structures is updated (referred to as the deformed configuration) and electrostatic analysis is performed on the deformed configuration to compute the surface charge densities. Once the surface charge density is known, the electrostatic forces are computed on the deformed configuration and transformed onto the initial configuration. Using the computed electrostatic forces a mechanical analysis is again performed in the initial configuration to recompute the structural

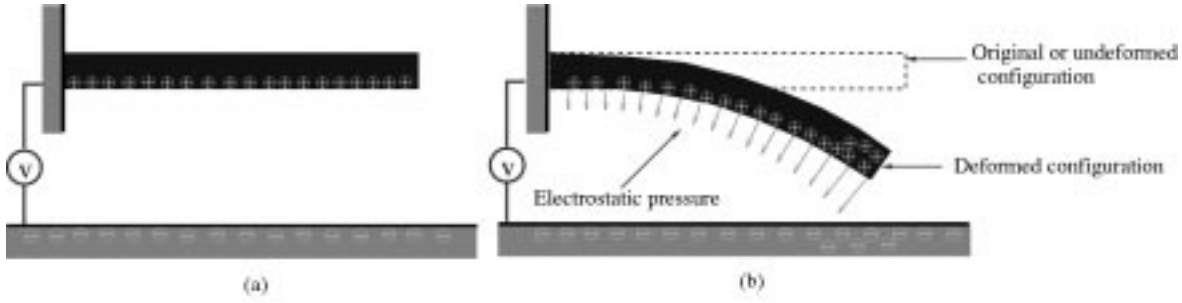

Fig. 1. Illustration of coupling in electrostatic MEMS through a simple example—a cantilever beam over a ground plane (a) applied voltage causes a charge distribution (b) the deformed structure with charge redistribution.

displacements. This procedure is repeated until an equilibrium position is reached. Typically, the mechanical analysis is performed by using a finite element method (FEM) [4] and the exterior electrostatic analysis is performed by using a boundary element method (BEM) [5].

A major difficulty with the approach described in Algorithm 1 is the need to update the geometry of the structures before an electrostatic analysis is performed during each iteration. This presents several problems—First, flat surfaces of the structures in the initial configuration can become curved due to deformation. This requires the development of complex integration schemes on curved panels [6] to perform electrostatic analysis. Second, when the structure undergoes very large deformation, remeshing the surface may become necessary before an electrostatic analysis is performed. Third, interpolation functions, used in many numerical methods, need to be recomputed whenever the geometry changes. Each of these issues significantly increases the computational effort making the self-consistent analysis of electrostatic MEMS an extremely complex and challenging task. If both mechanical and electrostatic analysis can be implemented using only the initial configuration, then the self-consistent analysis of electrostatically actuated devices would be radically simplified (see Algorithm 2). Hence, we ask the following fundamental question in this paper: Is it possible to perform electrostatic analysis on the initial configuration instead of using the deformed configuration? The answer is positive.

Algorithm 2 Procedure for coupled electromechanical analysis by using a Lagrangian approach for both mechanical and electrostatic analysis

repeat
1. Do mechanical analysis (on the undeformed geometry) to compute structural displacements
2. Compute surface charge density by electrostatic analysis (on the undeformed geometry)
3. Compute electrostatic forces (on the undeformed geometry)

until an equilibrium state is reached

II. Introduction

To restate the question posed at the end of the last section, consider a two conductor system as shown in Fig. 2. Ω_1 and Ω_2 denote the original geometry of conductor 1 and conductor 2, respectively, $d\,\Omega_1$ and $d\,\Omega_2$ denote the surface or boundary of conductor 1 and conductor 2, respectively, ω_1 denotes the deformed shape of conductor 1, ω_2 denotes the deformed shape of conductor 2, $d\omega_1$ and $d\omega_2$ denote the deformed surfaces of conductor 1 and conductor 2, respectively, and $\overline{\omega}$ is the domain exterior to ω_1 and ω_2. A potential of g_1 is applied on conductor 1 and a potential of g_2 is applied on conductor 2. The applied potentials do not change as the conductors undergo deformation or shape changes. The objective is to compute the surface charge density on the two conductors in the deformed position.

The question we pose in the paper is can we compute the surface charge densities on ω_1 and ω_2 by solving the electrostatic equations on the undeformed positions of the two conductors, i.e., using Ω_1 and Ω_2. As discussed in the previous section, electrostatic analysis using the undeformed position of the conductors can provide significant advantages. Borrowing ideas from the well known Lagrangian description of mechanics [8], we introduce a Lagrangian approach for electrostatic analysis. In the rest of the paper, a Lagrangian approach for electrostatic analysis refers to the solution of the electrostatic equations on the undeformed position of the conductors.

Even though we have used electrostatic MEMS as an example to motivate the need for Lagrangian electrostatic analysis, the approach described in the paper can be used to efficiently compute the surface charge densities or electrostatic forces whenever conductors undergo shape changes. The rest of paper is outlined as follows: Section III summarizes the deformed configuration approach to compute the electrostatic forces, Section IV describes the Lagrangian approach to compute the electrostatic forces acting on deformed structures, Section V compares the results obtained with deformed and Lagrangian approaches and conclusions are given in Section VI.

III. Electrostatic Analysis: Deformed Configuration Approach

We will deal with two-dimensional (2-D) electrostatic problems in this paper, but the approach can be extended trivially for three-dimensional (3-D) problems. Consider again the two conductor system shown in Fig. 2. The governing

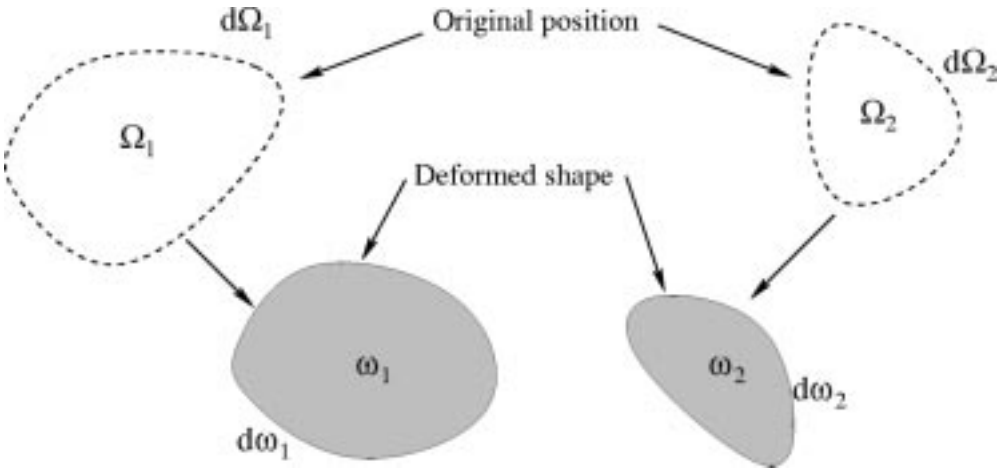

Fig. 2. A two-conductor electrostatic system.

equation along with the boundary conditions for the exterior electrostatics problem is given by [9]

$$\nabla^2\phi = 0 \qquad \text{in} \qquad \overline{\omega} \tag{1}$$

$$\phi = g_1 \qquad \text{on} \qquad d\omega_1 \tag{2}$$

$$\phi = g_2 \qquad \text{on} \qquad d\omega_2 \tag{3}$$

where $\overline{\omega}$ is the domain exterior to ω_1 and ω_2.

An efficient approach to treat exterior electrostatic problems is to use a boundary element method [5]. A boundary integral equation for the electrostatic problem is given by [10]

$$\phi(p) = \int_{d\omega} G(p,q)\sigma(q)\, d\gamma_q + C \tag{4}$$

$$\int_{d\omega} \sigma(q)\, d\gamma_q = C_T \tag{5}$$

where σ is the unknown surface charge density, p is the source point, q is the field point, G is the Green's function and $d\omega = d\omega_1 \cup d\omega_2$. In two-dimensions, $G(p, q) = -\ln|p-q|/(2\pi\epsilon)$, where $|p-q|$ is the distance between the source point p and the field point q, ϵ is the permitivity of the free space, C_T is the total charge of the system ($C_T = 0$) and C is an unknown variable which needs to be computed. The constant C is introduced because the potential ϕ at infinity is not zero for 2D electrostatics. Note that the variables in the governing equations (1)–(3) and the boundary-integral equations (4), (5) are written with respect to the deformed positions of the conductors. Hence, this approach is referred to as the deformed configuration approach.

A classical boundary element method is used to solve the boundary integral formulation given in equations (4), (5). In a classical boundary-element method, the surface is discretized into panels and the surface charge density is assumed to be constant on each panel. The centroid of each panel is taken as the collocation point and the value of the potential and the surface charge density at the collocation point represent the value of the potential and the surface charge density on the panel. The boundary integral equation for a source point p can be written as

$$\phi(p) = \sum_{k=1}^{K} \int_{d\omega_k} -\frac{1}{2\pi\epsilon} \ln|p-q_k|\sigma_k d\gamma_{q_k} + C \tag{6}$$

$$\sum_{k=1}^{K} \int_{d\omega_k} \sigma_k d\gamma_{q_k} = C_T \tag{7}$$

where K is the number of panels, $d\omega_k$ is the length of the kth panel, q_k is the field point on the kth panel and σ_k is the unknown charge density for the kth panel. Equations (6) and (7) can be rewritten in a matrix form as

$$\mathbf{M}\overline{\sigma} = \overline{\phi} \tag{8}$$

where $\mathbf{M}$ is a $(K+1)\times(K+1)$ coefficient matrix, $\overline{\phi}$ and $\overline{\sigma}$ are the $(K+1)\times 1$ right hand side and unknown vectors, respectively. The entries in the coefficient matrix are given by

$$\begin{cases} M(i,j) = \displaystyle\int_{d\omega_j} -\frac{1}{2\pi\epsilon}\ln|p_i - q_j| d\gamma_{q_j} & i,j = 1,\ldots,K \\ M(K+1,j) = \displaystyle\int_{d\omega_j} d\gamma_{q_j} & j = 1,\ldots,K \\ M(i,K+1) = 1 & i = 1,\ldots,K \\ M(K+1,K+1) = 0 \end{cases} \tag{9}$$

$$\overline{\phi} = \begin{Bmatrix} \phi_1 \\ \phi_2 \\ \cdot \\ \cdot \\ \cdot \\ \phi_K \\ C_T \end{Bmatrix} \qquad \overline{\sigma} = \begin{Bmatrix} \sigma_1 \\ \sigma_2 \\ \cdot \\ \cdot \\ \cdot \\ \sigma_K \\ C \end{Bmatrix}. \tag{10}$$

The $\overline{\phi}$ vector in (10) is known from the potential boundary conditions. The unknown surface charge density vector in (10) can be computed by solving the matrix problem in (8). Once the unknown surface charge densities are computed (note that these surface charge densities are on the deformed geometries), the

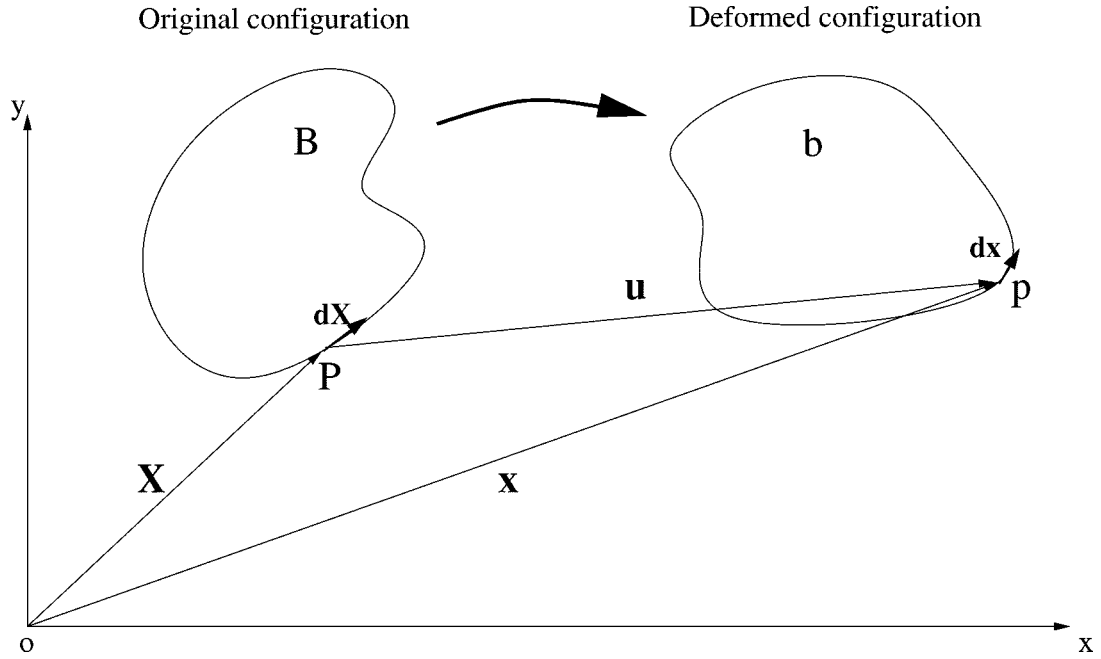

Fig. 3. Various configurations of a deformable body.

electrostatic force on a panel i on the deformed geometry is computed by [3]

$$\mathbf{h}_i = \frac{\sigma_i^2}{2\epsilon}\,\mathbf{n}_i \tag{11}$$

where $\mathbf{h}_i$ is the force per unit deformed area and $\mathbf{n}_i$ is the outward normal of panel i in the deformed configuration.

IV. Electrostatic Analysis: Lagrangian Approach

In the deformed configuration approach described in the previous section, boundary integral equations (4), (5) are defined and solved on the deformed geometry of the conductors. In this section, we introduce a Lagrangian formulation, where the boundary integral equations defined on deformed geometries are mapped to the initial or the original configuration of the conductors. The boundary integral equations with the Lagrangian description are then solved numerically in the initial configuration to compute the surface charge density and the electrostatic forces on the deformed configuration of the conductors.

A. Lagrangian Description in 2-D: Basic Concepts

When a material body is subjected to a force, either internal or external, its geometrical shape undergoes a change. As shown in Fig. 3, the initial configuration of a body is denoted by B (all quantities in the original configuration are denoted by capital letters) and the deformed configuration of the body is denoted by b (all quantities in the deformed configuration are denoted by lower case letters). Consider an infinitesimal segment on the boundary of B. Let P be the point where the infinitesimal boundary segment is directed from, $\mathbf{X}$ be the position vector of P and $d\mathbf{X}$ be the vector representing the infinitesimal boundary segment. When the body deforms to the deformed configuration b, particle P moves to p and its position changes to $\mathbf{x}$. The boundary segment $d\mathbf{X}$ in the initial configuration deforms to $d\mathbf{x}$ in the deformed configuration. Note that the boundary segment changes not only in length but also in direction when it deforms. The displacement from P to p is denoted by vector $\mathbf{u}$. The physical quantities in the deformed configuration can be expressed by the corresponding physical quantities in the initial configuration (Lagrangian description) as described as follows [8]:

$$\mathbf{x} = \mathbf{X} + \mathbf{u} \tag{12}$$

$$d\mathbf{x} = \mathbf{F}\,d\mathbf{X} \tag{13}$$

where $\mathbf{F}$ is the deformation gradient tensor given by

$$F_{ij} = \frac{\partial x_i}{\partial X_j} = \delta_{ij} + \frac{\partial u_i}{\partial X_j} \qquad i, j = 1, 2 \quad \text{for 2-D.} \tag{14}$$

The components of the position and displacement vectors are given by

$$\mathbf{x} = \begin{Bmatrix} x \\ y \end{Bmatrix} \quad \mathbf{X} = \begin{Bmatrix} X \\ Y \end{Bmatrix} \quad \mathbf{u} = \begin{Bmatrix} u \\ v \end{Bmatrix} \quad \text{for 2-D.} \tag{15}$$

In the initial configuration, the infinitesimal boundary segment $d\mathbf{X}$ can be represented by the product of its length $d\Gamma$ and its unit direction vector $\mathbf{T}$. Similarly, the boundary segment, $d\mathbf{x}$, in the deformed configuration can be represented by the product of its length $d\gamma$ and its unit direction vector $\mathbf{t}$.

$$d\mathbf{x} = d\gamma\mathbf{t} \tag{16}$$

$$d\mathbf{X} = d\Gamma\mathbf{T}. \tag{17}$$

By using the above relations, the geometry of a deformed structure can be expressed in terms of the geometry in the initial configuration and its deformation information.

B. Lagrangian Electrostatics

In the Lagrangian approach, we map the boundary integral equations in the deformed configuration, (4), (5), to the initial

configuration by representing each component in (4), (5) by its counterpart in the initial configuration.

The electric potential, ϕ, on the conductors and the dielectric constant ϵ of the medium are constants in the deformed and the initial configurations. Using (12) the Green's function in two dimensions, $G(p, q)$, can be rewritten as

$$G(p, q) = G(p(P), q(Q)) = -\frac{1}{2\pi\epsilon} \ln |P - Q + u_P - u_Q| \tag{18}$$

where P and Q are the source and field points in the initial configuration corresponding to the source and field points p and q in the deformed configuration, u_P and u_Q are the displacements of points P and Q, respectively. For coupled electromechanical analysis, these displacements are computed by a mechanical analysis. Using (13), (16), and (17) the length of an infinitesimal line element, $d\gamma$, in the deformed configuration is expressed in terms of the length of the corresponding line element, $d\Gamma$, in the initial configuration by

$$d\gamma \mathbf{t} = \mathbf{F}(d\Gamma \mathbf{T}). \tag{19}$$

Thus, we have

$$\begin{aligned}(d\gamma)^2 &= (d\gamma \mathbf{t}) \cdot (d\gamma \mathbf{t}) \\ &= [\mathbf{F}(d\Gamma \mathbf{T})] \cdot [\mathbf{F}(d\Gamma \mathbf{T})] \\ &= (d\Gamma)^2 (\mathbf{T} \cdot \mathbf{F}^T \mathbf{F} \mathbf{T}).\end{aligned} \tag{20}$$

The length of an infinitesimal line element in the deformed configuration can be written as

$$d\gamma = d\Gamma (\mathbf{T} \cdot \mathbf{F}^T \mathbf{F} \mathbf{T})^{1/2} \tag{21}$$

or,

$$d\gamma = d\Gamma (\mathbf{T} \cdot \mathbf{C} \mathbf{T})^{1/2} \tag{22}$$

where $\mathbf{C} = \mathbf{F}^T \mathbf{F}$ is the Green deformation tensor. At a specified point q,

$$d\gamma_q = d\Gamma_Q (\mathbf{T}(Q) \cdot \mathbf{C}(Q) \mathbf{T}(Q))^{1/2}. \tag{23}$$

Typically, the unknown quantity, such as the surface charge density, is approximated by using interpolation functions. In the deformed configuration, the surface charge density can be expressed as

$$\sigma(\mathbf{x}) = \sum_i N_i(\mathbf{x}) \sigma_i \tag{24}$$

where $\sigma(\mathbf{x})$ is the surface charge density at $\mathbf{x}$, σ_i is the value (constant) of the surface charge density at point i and $N_i(\mathbf{x})$ is the interpolation function of point i evaluated at $\mathbf{x}$. If the surface charge density needs to be computed in the initial configuration, then Equation (24) needs to be mapped to the initial configuration, i.e.,

$$\sigma(\mathbf{x}(\mathbf{X})) = \sum_i N_i(\mathbf{X}) \sigma_i \tag{25}$$

where $\sigma(\mathbf{x}(\mathbf{X}))$ is the surface charge density in the initial configuration, $N_i(\mathbf{X})$ is the interpolation function of point i evaluated at $\mathbf{X}$ in the initial configuration.

The Lagrangian form of the boundary integral equations given in (4), (5) is given by

$$\begin{aligned}\phi(P) = \int_{d\Omega} & G(p(P), q(Q)) \sigma(q(Q)) \\ & \cdot [\mathbf{T}(Q) \cdot \mathbf{C}(Q) \mathbf{T}(Q)]^{1/2} \, d\Gamma_Q + C\end{aligned} \tag{26}$$

$$\int_{d\Omega} \sigma(q(Q)) \, [\mathbf{T}(Q) \cdot \mathbf{C}(Q) \mathbf{T}(Q)]^{1/2} \, d\Gamma_Q = C_T. \tag{27}$$

By defining $\Xi(Q) = \sigma(q(Q)) \, [\mathbf{T}(Q) \cdot \mathbf{C}(Q) \mathbf{T}(Q)]^{1/2}$ as the charge density per unit undeformed surface area, (26), (27) can be rewritten as

$$\phi(P) = \int_{d\Omega} G(p(P), q(Q)) \Xi(Q) d\Gamma_Q + C \tag{28}$$

$$\int_{d\Omega} \Xi(Q) \, d\Gamma_Q = C_T. \tag{29}$$

Observe that the integrals are now defined over surfaces ($d\,\Omega$) in the initial configuration and all the quantities inside the integrals are also defined using the initial configuration. Substituting (24) and the Green's function given in (18), (26), (27) can be rewritten as

$$\begin{aligned}\phi(P) = \int_{d\Omega} & -\frac{1}{2\pi\epsilon} \ln |P - Q + u_P - u_Q| \left[\sum_i N_i(\mathbf{X}) \sigma_i \right] \\ & \cdot [\mathbf{T}(Q) \cdot \mathbf{C}(Q) \mathbf{T}(Q)]^{1/2} \, d\Gamma_Q + C\end{aligned} \tag{30}$$

$$\int_{d\Omega} \left[\sum_i N_i(\mathbf{X}) \sigma_i \right] [\mathbf{T}(Q) \cdot \mathbf{C}(Q) \mathbf{T}(Q)]^{1/2} \, d\Gamma_Q = C_T. \tag{31}$$

If the unknown surface charge density is assumed constant on each panel, then the Lagrangian form given in (30), (31) can be rewritten as

$$\begin{aligned}\phi(P) = \sum_{k=1}^{K} \int_{d\Omega_k} & -\frac{1}{2\pi\epsilon} \ln |P - Q_k + u_P - u_{Q_k}| \sigma_k \\ & \cdot [\mathbf{T}(Q_k) \cdot \mathbf{C}(Q_k) \mathbf{T}(Q_k)]^{1/2} \, d\Gamma_{Q_k} + C\end{aligned} \tag{32}$$

$$\sum_{k=1}^{K} \int_{d\Omega_k} \sigma_k \, [\mathbf{T}(Q_k) \cdot \mathbf{C}(Q_k) \mathbf{T}(Q_k)]^{1/2} \, d\Gamma_{Q_k} = C_T \tag{33}$$

where K is the number of panels, $d\Omega_k$ is the length of kth panel, Q_k is the field point on the kth panel and σ_k is the constant charge density for kth panel. Equations (32), (33) can be rewritten in a matrix form as

$$\overline{\mathbf{M}} \overline{\sigma} = \overline{\phi} \tag{34}$$

where $\overline{\mathbf{M}}$ is $(K+1) \times (K+1)$ coefficient matrix, $\overline{\phi}$ and $\overline{\sigma}$ are $(K+1) \times 1$ right-hand side and unknown vector, respectively. The entries of the coefficient matrix are given by (35) and (36) as shown at the bottom of the next page. By substituting the potential boundary conditions on the conductors and the total charge into (36), the surface charge density on the panels can be computed from (34). Comparing (35) with (9), an extra term $[\mathbf{T} \cdot \mathbf{C} \mathbf{T}]^{1/2}$ needs to be computed in the Lagrangian approach. The Green deformation tensor $\mathbf{C}$ is a 2×2 matrix in 2-D and a

3×3 matrix in 3-D. Similarly, $\mathbf{T}$ is a 2×1 vector in 2-D and a 3×1 vector in 3-D. Since these are small matrices the additional computational cost is minor and is typically 5% more than the cost required to evaluate (9).

Once the surface charge densities on the deformed configuration are computed, the electrostatic forces acting on the deformed geometry can again be computed by using (11). By transforming the electrostatic pressure on the deformed configuration to the initial configuration, $\mathbf{h}\,ds = \mathbf{H}\,dS$, and applying the Nanson's Law [8], $(ds)\mathbf{n} = J(dS)\mathbf{F}^{-T}\mathbf{N}$, the electrostatic force per unit undeformed area in the initial configuration (denoted by $\mathbf{H}_i$) can is given by

$$\mathbf{H}_i = \frac{\sigma_i^2}{2\epsilon}\, J_i \mathbf{F}_i^{-T} \mathbf{N}_i \tag{37}$$

where ds and dS are the infinitesimal deformed and undeformed area, respectively, J is the determinant of $\mathbf{F}$, $\mathbf{H}_i$ and $\mathbf{N_i}$ are the electrostatic force vector and the outward normal on panel i in the initial configuration, respectively.

V. Numerical Results

Numerical results are presented for several two-dimensional two conductor problems using the classical boundary-element method. A potential difference is created between the two conductors and the surface charge density is computed by both the deformed configuration approach and the original configuration (or the Lagrangian) approach. For simplicity, the permitivity of the free space in (4) is set to be 1 and $C_T = 0$ for all the examples.

As a first example, we consider two 1×1 square conductors separated by a distance of 2 units along the x-axis. A potential of 1 volt is applied on the left conductor and the right conductor is grounded. The left conductor is subjected to a shear deformation as shown in Fig. 4(a). The dashed line represents the initial configuration of the left conductor and the solid shape is the deformed configuration. Note that the right conductor is fixed and does not undergo any deformation. The displacement field of the deformed conductor is given by

$$\begin{cases} u = Y \\ v = 0 \end{cases} \tag{38}$$

where u is the x-component of the displacement and v is the y-component of the displacement. The objective is to compute the surface charge density on the two conductors when the left conductor undergoes shear deformation.

In the deformed configuration approach [summarized in (6) and (7)], the deformed position of the left conductor and the right conductor are each discretized into 80 panels to compute the surface charge density. In the Lagrangian approach [summarized in (32), (33)], the original position [shown dashed in Fig. 4(a)] of the left conductor and the right conductor are each discretized into 80 panels to compute the surface charge density. The charge density distributions on the conductors obtained by the Lagrangian as well as by the deformed configuration approach, are identical. This distribution is shown in Fig. 4(a).

The geometry of the second example is identical to the geometry considered in the first example. However, in the second example we assume that the left conductor undergoes a rotation instead of a shear deformation. The initial and the deformed configurations of the second problem are shown in Fig. 4(b). The dashed line again represents the original position and the solid shape is the deformed configuration. The displacement field of the deformed (or left) conductor is given by

$$\begin{cases} u = \left(\dfrac{\sqrt{2}}{2} - 1\right) X - \dfrac{\sqrt{2}}{2} Y \\ v = \dfrac{\sqrt{2}}{2} X + \left(\dfrac{\sqrt{2}}{2} - 1\right) Y. \end{cases} \tag{39}$$

The surface charge density is again computed by the deformed configuration and the Lagrangian approaches. As shown

$$\begin{cases} \overline{M}(i,\, j) = \displaystyle\int_{d\Omega_j} -\frac{1}{2\pi\epsilon} \ln |P_i - Q_j + u_{P_i} - u_{Q_j}|\, [\mathbf{T}(Q_j) \cdot \mathbf{C}(Q_j)\mathbf{T}(Q_j)]^{1/2}\, d\Gamma_{Q_j} & i, j = 1, \ldots, K \\ \overline{M}(K+1,\, j) = \displaystyle\int_{d\Omega_j} [\mathbf{T}(Q_j) \cdot \mathbf{C}(Q_j)\mathbf{T}(Q_j)]^{1/2}\, d\Gamma_{Q_j} & j = 1, \ldots, K \\ \overline{M}(i,\, K+1) = 1 & i = 1, \ldots, K \\ \overline{M}(K+1,\, K+1) = 0 \end{cases} \tag{35}$$

$$\overline{\phi} = \begin{Bmatrix} \phi_1 \\ \phi_2 \\ \cdot \\ \cdot \\ \cdot \\ \phi_K \\ C_T \end{Bmatrix} \qquad \overline{\sigma} = \begin{Bmatrix} \sigma_1 \\ \sigma_2 \\ \cdot \\ \cdot \\ \cdot \\ \sigma_K \\ C \end{Bmatrix} \tag{36}$$

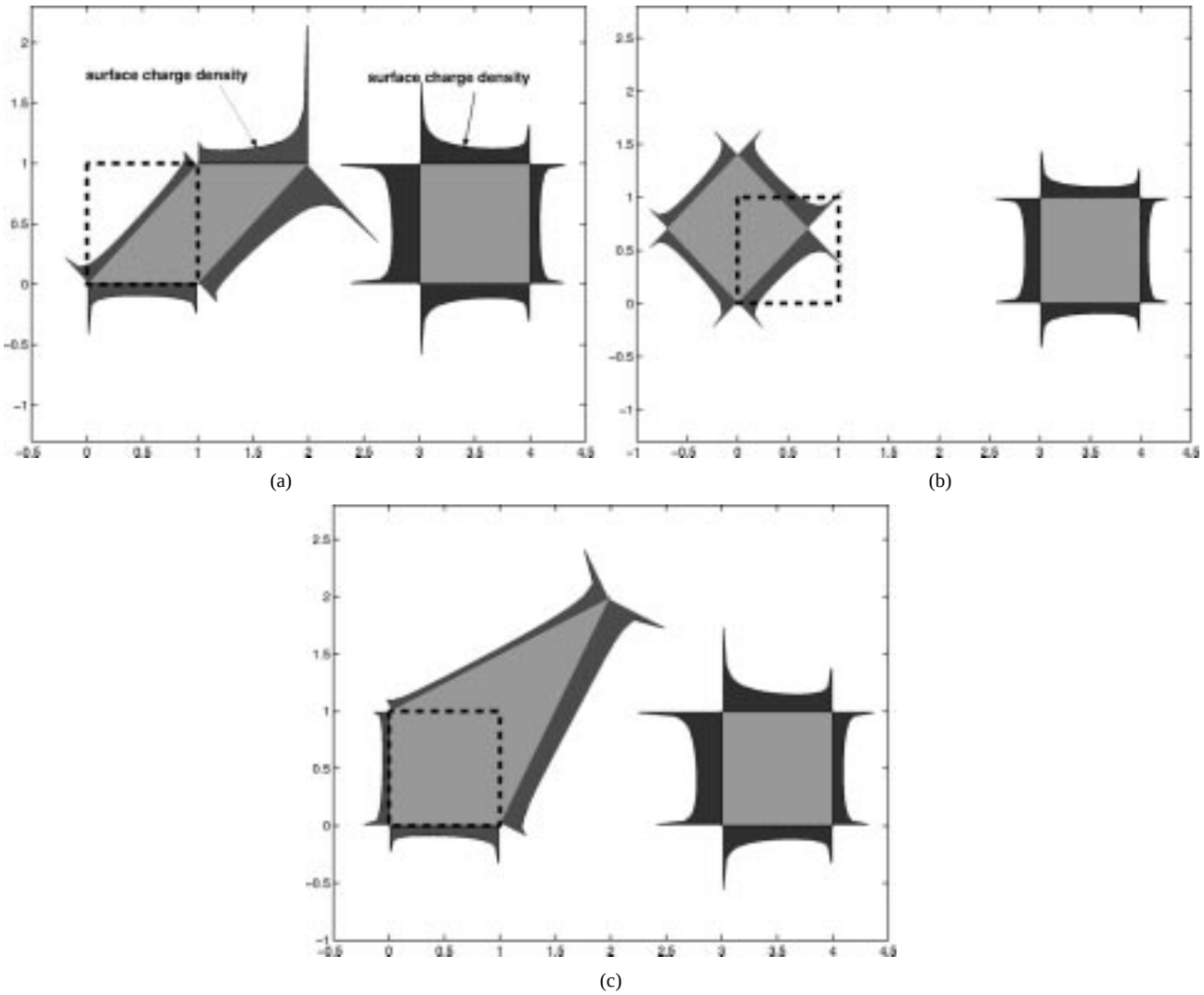

Fig. 4. Surface charge densities for the two conductor example (a) The left conductor is subjected to a shear deformation (b) The left conductor is subjected to a rotation (c) The left conductor is subjected to a stretch. Note that the surface charge densities computed by the deformed as well as by the Lagrangian approach are identical (both plots coincide).

in Fig. 4(b), the surface charge density computed by both approaches is identical.

In the third example, we again consider the two conductor system. In this case we assume that the displacement field of the left conductor is given by

$$\begin{cases} u = XY \\ v = XY. \end{cases} \tag{40}$$

The original and the deformed configurations of the third example are shown in Fig. 4(c). The surface charge density is again computed by both deformed configuration and Lagrangian approaches and identical results are obtained as shown in Fig. 4(c).

In the next example, we consider two rectangular conductors or beams of dimensions 4×1 as shown in Fig. 5. The distance between the two beams is 4 units along the y-axis. A potential of 1 volt is applied on the top conductor and the bottom conductor is grounded. The bottom conductor is fixed. The left end of the top conductor is fixed and the displacement of the top beam is given by

$$\begin{cases} u = \frac{1}{100}\left(\frac{9}{4}Y^3 - 3X^2Y + \frac{3}{2}X^2 - \frac{27}{8}Y^2 \right. \\ \qquad \left. + 24XY - 12X + \frac{9}{8}Y\right) \\ v = \frac{1}{100}\left(X^3 + \frac{3}{4}XY^2 - 12X^2 - 3Y^2 \right. \\ \qquad \left. - \frac{3}{4}XY - \frac{9}{8}X + 3Y - \frac{3}{4}\right). \end{cases} \tag{41}$$

The original and the deformed configurations of the system are shown in Fig. 5. The problem is solved by using the Lagrangian and the deformed configuration approaches. The surface charge density computed by the Lagrangian approach is shown in Fig. 5(a) and the surface charge density computed by the deformed configuration approach is shown in Fig. 5(b). The results look identical, but there is a small difference in the solutions obtained by the two approaches. The small error arises because of the geometrical approximations involved in the deformed configuration approach. When a conductor deforms or changes shape, the surfaces become curved. When curved surfaces are approximated by straight panels, numerical errors

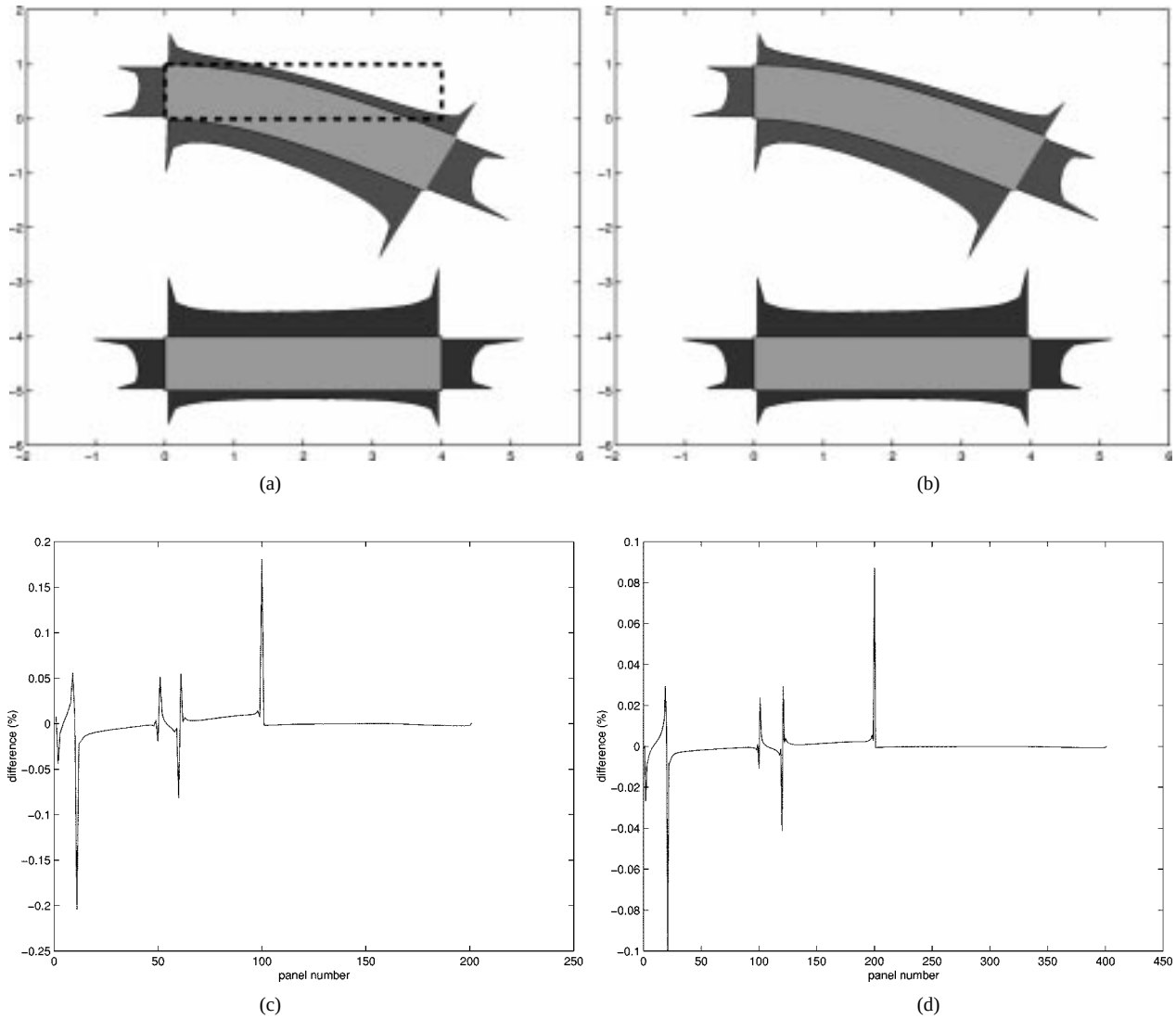

Fig. 5. Two conductor system with a small displacement for the top conductor (a) surface charge densities computed with the Lagrangian approach (b) surface charge densities computed with the deformed configuration approach (c) Difference in surface charge density between the two approaches when 100 panels are used for each conductor (d) Difference in surface charge density between the two approaches when 200 panels are used for each conductor.

can be introduced into the deformed configuration approach. To verify this observation, a refinement study is performed to investigate the difference in the solution between the two approaches. Each conductor is first discretized into 100 panels and the maximum difference between the two approaches is found to be 0.2%. The error due to the integration on the curved surfaces can be found between the peak differences. When the conductors are discretized into 200 panels each, the maximum difference reduced to 0.1% and the integration error is also reduced. The error plots are shown in Fig. 5(c) and (d). The use of more panels to approximate curved surfaces reduces the integration error in the deformed configuration approach and hence the results are closer to the Lagrangian approach. From this example, we can conclude that the Lagrangian approach is more accurate as all the integrations are performed in the initial configuration.

The final example is a two conductor system containing two 8×1 rectangular beams. The distance between the two conductors is 8 units along the y-axis. A potential of 1 volt is applied on the top conductor and the bottom conductor is grounded. The bottom conductor is fixed and so is the left end of the top conductor. The top conductor is given a large displacement as shown in Fig. 6. The surface charge densities computed with the two approaches are shown in Fig. 6. Once again we observe that there are small differences in the two solutions. Since the surfaces are curved in the deformed configuration, the use of straight panels introduces numerical integration error in the deformed configuration approach. When the conductors are discretized into 50 panels each, we observe that the maximum error is about 1%. When 100 panels are used, the error reduces to 0.5%. The error plots are shown in Fig. 6(c) and (d).

VI. Conclusion

In this paper, we have introduced a Lagrangian approach to compute electrostatic forces on deformable conductors. This approach is mathematically equivalent to the conventional deformed configuration approach. However, the Lagrangian approach possesses several advantages: 1) it does not require any update of the geometry of the structures 2) it eliminates

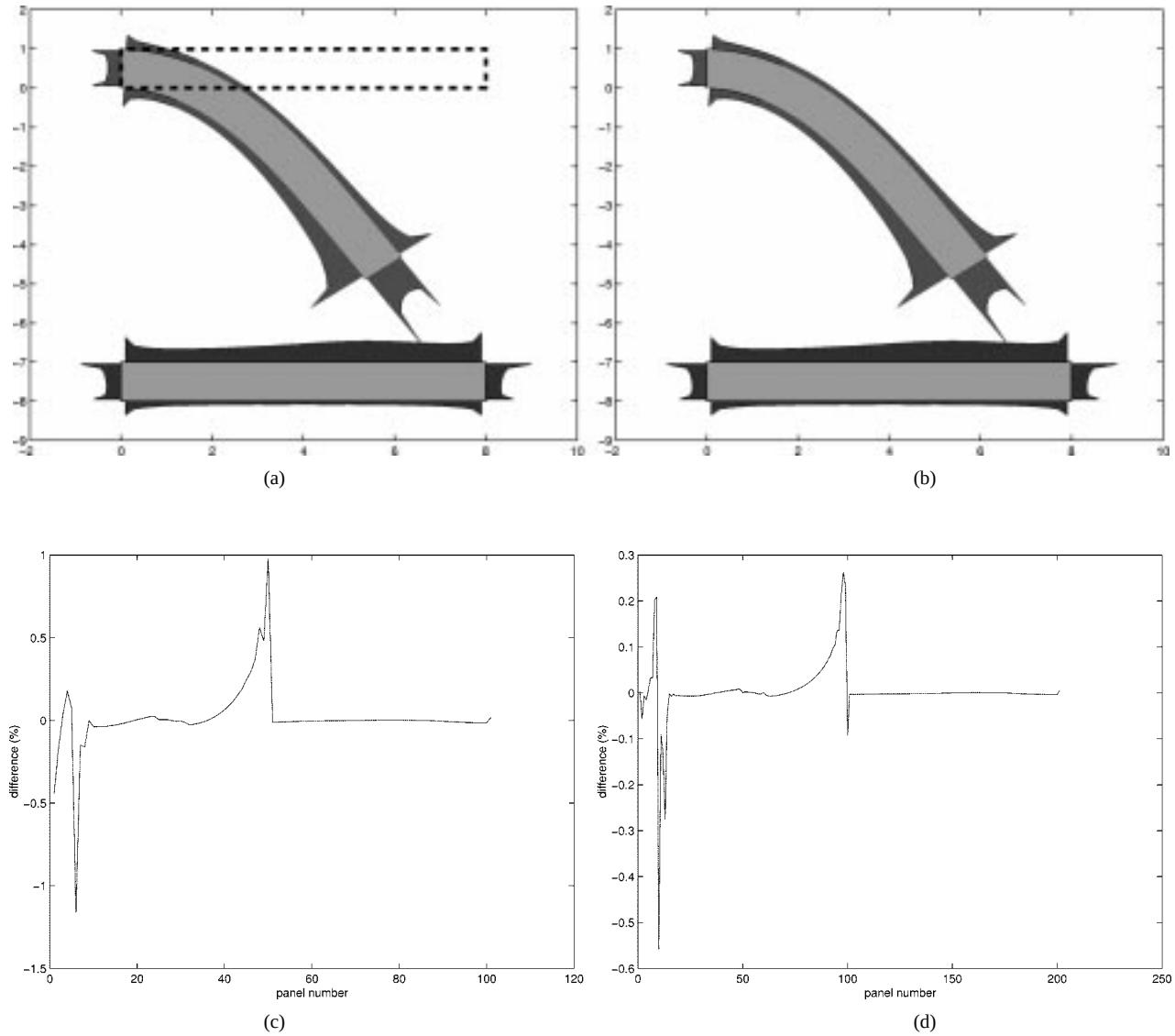

Fig. 6. Two conductor system with large displacement for the top conductor (a) surface charge density computed with the Lagrangian approach (b) surface charge density computed with the deformed configuration approach. (c) Difference in surface charge density between the two approaches when 50 panels are used for each conductor. (d) Difference in surface charge density between the two approaches when 100 panels are used for each conductor.

integration error that arises when flat panels are used to approximate curved surfaces 3) interpolation functions need not be re-computed whenever a structure undergoes a shape change. Therefore, the Lagrangian approach is an accurate and efficient way to compute electrostatic forces on deformable MEMS. The combination of a Lagrangian approach for electrostatic analysis with a Lagrangian approach for mechanical analysis can radically simplify coupled electromechanical analysis.

REFERENCES

[1] S. D. Senturia, R. M. Harris, B. P. Johnson, S. Kim, K. Nabors, M. A. Shulman, and J. K. White, "A computer-aided design system for microelectromechanical systems," *J. Microelectromech. Syst.*, vol. 1, no. 1, pp. 3–13, 1992.

[2] J. R. Gilbert, R. Legtenberg, and S. D. Senturia, "3D coupled electromechanics for MEMS: Applications of CoSolve-EM," in *Proc. MEMS 1995*, 1995, pp. 122–127.

[3] N. R. Aluru and J. White, "An efficient numerical technique for electromechanical simulation of complicated microelectromechanical structures," *Sens. Actuators, Phys. A*, vol. 58, pp. 1–11, 1997.

[4] T. J. R. Hughes, *The Finite Element Method*: Prentice-Hall, 1987.

[5] J. H. Kane, *Boundary Element Analysis in Engineering Continuum Mechanics.* Englewood Cliffs, NJ: Prentice-Hall, 1994.

[6] X. Wang, J. N. Newman, and J. White, "Robust algorithms for boundary-element integrals on curved surfaces," in *Proc. 1st International Conference on Modeling and Simulation of Microsystems, Semiconductors, Sensors and Actuators (MSM 00)*, 2000, pp. 473–476.

[7] L. M. Delves and J. L. Mohamed, *Computational Methods for Integral Equations*, U.K.: Cambridge University Press, 1985.

[8] D. S. Chandrasekharaiah and L. Debnath, *Continuum Mechanics.* New York: Academic, 1994.

[9] J. D. Jackson, *Classical Electrodynamics*, 3rd ed. New York: Wiley, 1999.

[10] F. Shi, P. Ramesh, and S. Mukherjee, "On the application of 2D potential theory to electrostatic simulation," *Commun. Numerical Meth. Eng.*, vol. 11, pp. 691–701, 1995.

[11] S. P. Timoshenko and J. N. Goodier, *Theory of Elasticity*. New York: McGraw-Hill, 1982.

Gang Li received the B.S. and M.Eng. degrees in mechanical engineering from Tongji University, Shanghai, P.R. China, in 1993 and 1996, respectively. He received the M.Asc. degree in mechanical engineering from Dalhousie University, Halifax, Canada, in 1999. He is currently working towards the Ph.D. degree in mechanical engineering at the University of Illinois at Urbana-Champaign (UIUC).

His research interests include computational analysis and design of MEMS and numerical methods in engineering.

N. R. Aluru (M'00) received the B.E. degree with honors and distinction from the Birla Institute of Technology and Science, Pilani, India, in 1989, the M.S. degree from Rensselaer Polytechnic Institute, Troy, NY, in 1991, and the Ph.D. degree from Stanford University, Stanford, CA, in 1995.

He was a Postdoctoral Associate at the Massachusetts Institute of Technology (MIT), Cambridge, from 1995 to 1997. In 1998, he joined the Department of General Engineering, university of Illinois, Urbana-Champaign (UIUC) as an Assistant Professor. He is affiliated with the Beckman Institute for Advanced Science and Technology, the Department of Electrical and Computer Engineering, and the Department of Mechanical and Industrial Engineering at UIUC. His current research interests are in the areas of computational methods, MEMS/NEMS, micro/nano fluidics, Bio-MEMS, and bionanotechnology.

Dr. Aluru received the 1999 National Science Fooundation CAREER Award, the 1999 NCSA Faculty Fellowship, and a 2001 CMES Distinguished Young Author Award.